Zic-associated holoprosencephaly: zebrafish Zic1 controls midline formation and forebrain patterning by regulating Nodal, Hedgehog, and retinoic acid signaling

Daniel Maurus and William A. Harris[1]

Department of Physiology, Development, and Neuroscience, University of Cambridge, Cambridge CB2 3DY, United Kingdom

Holoprosencephaly (HPE) is the most frequently observed human embryonic forebrain defect. Recent evidence indicates that the two major forms of HPE, classic HPE and midline interhemispheric (MIH) HPE, are elicited by two different mechanisms. The only gene known to be associated with both forms of HPE is *Zic2*. We used the zebrafish *Danio rerio* as a model system to study Zic knockdown during midline formation by looking at the close homolog Zic1, which is expressed in an overlapping fashion with Zic2. Zic1 knockdown in zebrafish leads to a strong midline defect including partial cyclopia due to attenuated Nodal and Hedgehog signaling in the anterior ventral diencephalon. Strikingly, we were able to show that Zic1 is also required for maintaining early forebrain expression of the retinoic acid (RA)-degrading enzyme *cyp26a1*. Zic1 LOF leads to increased RA levels in the forebrain, subsequent ventralization of the optic vesicle and down-regulation of genes involved in dorsal BMP signaling. Repression of BMP signaling in dorsal forebrain has been implicated in causing MIH HPE. This work provides a mechanistical explanation at the molecular level of why Zic factors are associated with both major forms of HPE.

[*Keywords*: Zic2; midline interhemispheric holoprosencephaly; Sonic hedgehog; Cyclops; Cyp26a1; retina]

Supplemental material is available at http://www.genesdev.org.

Received December 8, 2008; revised version accepted April 23, 2009.

Holoprosencephaly (HPE) is the most common forebrain malformation during human embryonic development, with an estimated incidence of one in 5000–10,000 live births (Fernandes and Hébert 2008). In induced abortions, the rate is much higher, at one in 250 (Matsunaga and Shiota 1977). HPE is characterized by an incomplete separation of the bilateral hemispheres of the telencephalon due to incomplete formation of midline structures (for review, see Cohen 2006; Fernandes and Hébert 2008). In severe cases of HPE, separation of the eye field fails, resulting in cyclopia.

In classic HPE, components of the TGFβ/Nodal and Hedgehog pathway were found to be mutated most frequently. Activity of these pathways in axial mesoderm and anterior ventral neuroectoderm is crucial for the formation of ventral neural midline tissue and bilateral splitting of the early eye field (for review, see Bertrand and Dahmane 2006). TGFβ/Nodal signaling acts upstream of the Sonic hedgehog (Shh) pathway during midline formation, as has been demonstrated in zebrafish and mouse (Lowe et al. 2001; Rohr et al. 2001). A second class of HPE is midline interhemispheric (MIH) HPE, in which development of ventral forebrain can be normal but development of the dorsal roofplate of the forebrain is impaired, leading to a milder form of HPE (Fernandes and Hébert 2008). BMP signaling has been shown to play an important role during dorsal midline development (Fernandes et al. 2007).

The only gene known to be associated with classic HPE as well as MIH HPE is *zic2* (Brown et al. 1998; Nagai et al. 2000; Brown et al. 2001). A recent study in mice, however, suggests that Zic2 might be required during mid-gastrulation in the organizer region as an arrest in the development of the prechordal plate can be observed in $Zic2^{Ku/Ku}$ mutants (Warr et al. 2008). This is before Hedgehog signaling begins and suggests that Zic2 may function upstream of Hedgehog. In *Xenopus*, embryos depleted of maternal Zic2 do not show a midline defect,

[1]**Corresponding author.**
E-MAIL harris@mole.bio.cam.ac.uk; FAX 441223-333840.
Article is online at http://www.genesdev.org/cgi/doi/10.1101/gad.517009.

although injection of a truncated Zic2 (tZic2) construct in such embryos resulted in cyclopic embryos, indicating that tZic2 may interfere with zygotic Zic2 or other Zic proteins during later stages of development (Houston and Wylie 2005).

Loss of function (LOF) of zebrafish Zic2a, the closest homolog of mammalian Zic2, does not seem to interfere with midline development. Expression of Shh target genes like *ptc1*, *gli1*, and *nkx2.2a* are unaffected, suggesting that Zic2a and Hedgehog signaling act in parallel during zebrafish forebrain development (Sanek and Grinblat 2008). Although there is the possibility that Zic2a plays a different role from that of its mammalian counterpart Zic2, it is also possible that redundancy masks the function of Zic2a during zebrafish midline development. This possibility needs to be considered seriously as expression of *zic* genes is highly overlapping during gastrulation and neurulation in zebrafish and because double knockout of Zic1/Zic3 or Zic2/Zic3 in mice unmasks further roles for Zic factors, which are not evident from single knockouts (Inoue et al. 2007a,b). For example, double knockout of *zic1* and *zic3* revealed a role for *zic1* during medial forebrain development (Inoue et al. 2007a). In zebrafish, the function of Zic1 has so far only been addressed in the dorsal hindbrain (Elsen et al. 2008), yet *zic1* shows further overlapping expression with *zic2a* in anterior neural tissue (Grinblat and Sive 2001). We, therefore, wished to know whether the combined LOF of Zic2a and closely related Zic1 (Grinblat et al. 1998; Rohr et al. 1999) would result in a midline phenotype.

The work reported here starts by showing that the combined Zic1 and Zic2a LOF causes forebrain midline defects in zebrafish embryos. Further experiments reveal that knockdown of Zic1 by itself causes a strong midline phenotype including partial cyclopia. As *zic1* expression starts during late midgastrulation in anterior neural tissue only, we can exclude the possibility of compromised organizer/prechordal plate development. Analysis of marker genes for optic stalk and forebrain reveals strongly reduced expression of genes promoting proximal–ventral fate indicative of reduced activity of ventral midline signals, yet we also find a ventralization of the optic vesicle. Insight into this complex phenotype comes from our demonstration that Zic1 LOF decreases Nodal and Hedgehog signaling, on the one hand (leading to reduced expression of optic stalk marker genes), and increases Retinoic acid (RA) signaling, on the other hand (leading to a ventralization of the optic vesicle). The reduction of Nodal and Hedgehog signaling is due to reduced expression of the ligands Cyclops and Sonic hedgehog (Shh), while the increase in RA signaling is due to reduced expression of the anteriorly expressed RA-degrading enzyme Cyp26a1. Rescue experiments suggest that Zic1 is upstream of Nodal, Hedgehog, and RA signaling and imply that knockdown of Zic1 independently impairs both ventral (Shh) and dorsal (BMP) midline signaling, and allow an interpretation of why *zic* genes are associated with classic HPE as well as MIH HPE.

Results

Loss of Zic1 function causes forebrain midline defects

Mutation of *zic2* causes HPE in humans and in the mouse model. LOF of the zebrafish homolog Zic2a does not lead to occurrence of a forebrain midline phenotype, possibly because other Zic factors act redundantly (Sanek and Grinblat 2008). An interesting candidate gene is *zic1*. *Zic1* expression can be detected in the prospective forebrain region during gastrulation from 70% epiboly onward and stays robust in the prospective ventral forebrain until the five- to six-somite stage (Supplemental Fig. S1; Grinblat et al. 1998; Rohr et al. 1999; Varga et al. 1999). To test if zebrafish Zic2a and Zic1 act redundantly, we knocked down expression of both genes. As the previously published Zic1 translation-blocking morpholino (Elsen et al. 2008) caused a delay in gastrulation at the effective dose (D Maurus and WA Harris, unpubl.), we designed a new Zic1 splice-blocking morpholino (Z1MO) (Supplemental Fig. S3; see the Materials and Methods) that does not affect gastrulation movements. Identification of midline defects was in the first instance based on morphology of optic stalk and vesicle, as formation of optic tissue is a well-studied readout for the early detection of defective midline formation. Zebrafish embryos were examined after 72 h post-fertilization (hpf) when formation of eyes and retinal pigmented epithelium (RPE) allows easy examination of embryos for eye defects and defective midline development. Combined injection of morpholino oligonucleotides against *zic2a* (Z2aMO, 5 ng) and *zic1* (Z1MO, 2 ng) strikingly caused defective development of midline structures, whereas separate injections of both morpholinos at respective concentrations caused them only in the case of Z1MO minor midline defects at a low frequency (Supplemental Fig. S2).

As injection of 2 ng of Z1MO elicited midline defects, we tested if higher concentrations of Z1MO might increase the severity and frequency of such defects. Indeed, embryos injected with 3–4 ng of Z1MO display a range of midline phenotypes (Fig. 1). In most severely affected embryos, the RPE of both eyes is fused in the midline, leading to partial cyclopia (Fig. 1A,G). This fusion was observed only dorsally, not ventrally, and a complete fusion of both eyes (full cyclopia) was not observed. Less severely affected embryos frequently display an expansion of RPE into the optic stalk (Fig. 1B). Weakly affected embryos show pronounced (Fig. 1C,C′,G) or less pronounced coloboma (Fig. 1D,D′,G), an incomplete closure of the choroid fissure of the eye. Coloboma and conversion of optic stalk tissue into retinal tissue have been reported as well in mice and zebrafish devoid of Vax1 and Vax2 (Take-uchi et al. 2003; Mui et al. 2005), pointing toward a misregulation of ventral specification of the optic vesicle in Zic1 morphants during early stages of development.

To confirm specificity of the phenotype, we tried to rescue the Z1MO-elicited phenotype by coinjection of *zic1* mRNA. Indeed, embryos coinjected with *zic1* mRNA display a reduction in occurrence of midline

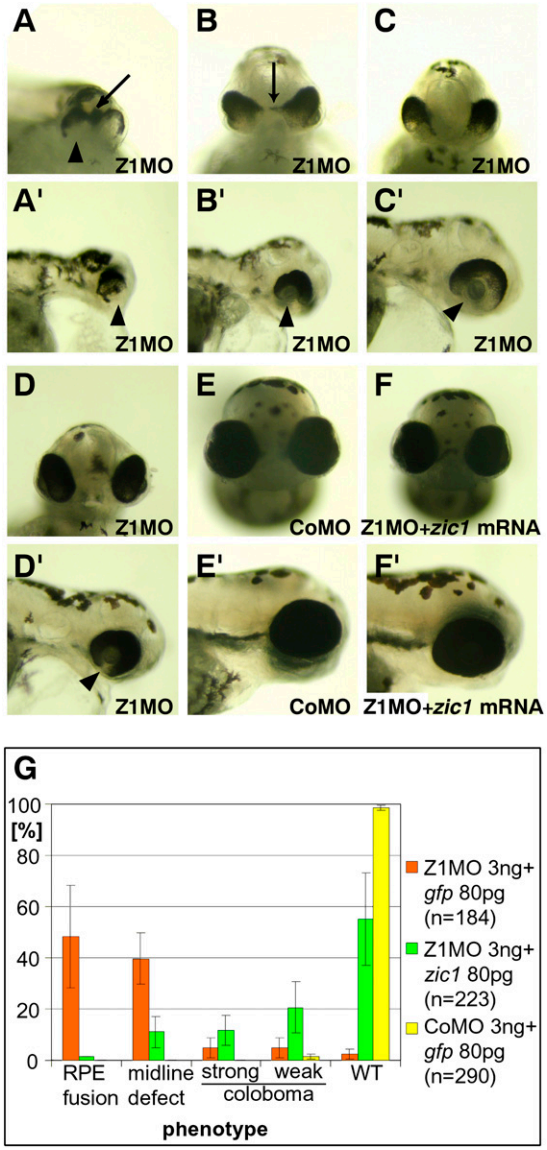

Figure 1. Zic1 LOF elicits defective development of the embryonic midline and the eye at 72 hpf. (*A–F*) Frontal view. (*A′–F′*) Lateral view with rostral to the *right*. (*A*,*A′*) Severely affected embryos show dorsal fusion of RPE of both eyes (arrow) indicating disturbed midline development. RPE is missing in the ventral eye (arrowhead). (*B*,*B′*) Less severely affected embryos show an expansion of RPE into the optic stalk domain (arrow). Massive coloboma can be observed in the ventral eye (arrowhead). (*C*,*C′*) In weakly affected embryos, coloboma is still pronounced (arrow). (*D*,*D′*) Morphants with a very weak phenotype show weak but clearly detectable coloboma (arrowhead). (*E*,*E′*) Control morpholino-injected embryo. (*F*,*F′*) Coinjection of Zic1 morphants with *zic1* mRNA rescues the phenotype. (*G*) Quantification of frequency of described phenotypes and rescue experiment. Most embryos injected with Z1MO show RPE fusion and midline defects, whereas most morphants coinjected with *zic1* mRNA show only coloboma or no phenotype. (WT) Wild type.

defects. The frequency of severe midline defects is massively reduced (Fig. 1F,G). We therefore conclude the midline phenotype elicited by Z1MO (3–4 ng) to be specific. As knockdown of Zic1 by itself caused a significant midline defect, we confined our further experiments on the role of *zic* genes during midline development to the study of Zic1 function.

Analysis of Z1MO-injected embryos earlier reveals that from the eight- to nine-somite stage on Zic1 LOF causes cell death in the optic vesicle and prospective diencephalon (Supplemental Fig. S4A). To exclude the possibility of nonspecific necrosis elicited by Z1MO injection, we rescued cell death by *zic1* mRNA coinjection (Supplemental Fig. S4D). As rescue proved cell death to be specifically caused by Zic1 LOF, we assumed cell death to be caused by apoptosis. To confirm this, we stained Z1MO-injected embryos with an antibody against activated caspase-3 (Negron and Lockshin 2004). Stained domains match domains in which cell death occurs (Supplemental Fig. S4F). As apoptosis could contribute to the observed midline phenotype, we rescued apoptosis through coinjection of *bcl2* mRNA (Supplemental Fig. S4H,J), a factor antagonizing apoptosis (Langenau et al. 2005), and analyzed the resulting phenotype after 3 d. Analysis indicates that rescue of apoptosis does not lead to rescue of midline defects (Supplemental Fig. S4J). The observed midline defect is therefore not caused by apoptosis; rather, the apoptosis may be caused by an earlier event leading to occurrence of the midline defect around the tailbud/one-somite stage (see below).

We wondered if formation of the telencephalic midline, which plays an important role in the separation of the two hemispheres, is also disturbed in Zic1 morphants. At 26 hpf, the telencephalon of Zic1 morphants displays severely disorganized tissue (Supplemental Fig. S5). Marker analyses indicate that *fgf8* expression is strongly up-regulated and expressed ectopically in the telencephalon (Supplemental Fig. S5A,B′), and expression of other early telencephalic marker genes *emx1*, *fezl*, and *er81* are partially affected (Supplemental Fig. S5C–H).

Zic1 acts upstream of Sonic hedgehog target genes

We examined the expression of marker genes for ventral specification of the forebrain and optic primordium by whole-mount in situ hybridization (WMISH) to see if occurrence of the phenotype is preceded by a change in marker gene expression.

Vax1 and *Vax2* are expressed in overlapping domains encompassing the optic stalk, preoptic area, and ventral retina. Loss of Vax1 and Vax2 function in mice and zebrafish causes coloboma (Take-uchi et al. 2003; Mui et al. 2005), similar to the phenotype observed in weakly affected Zic1 morphants. In Zic1 morphants, the expression of both genes is strongly reduced. *Vax1* expression is strongly reduced in all expression domains (Fig. 2A; Supplemental Table S1), whereas *vax2* expression is reduced more specifically in the ventral retina, the most distal expression domain (Fig. 2C). Reduction of these marker genes is reminiscent of studies in which midline signals like Hedgehog were compromised (Take-uchi et al. 2003; Lupo et al. 2005). As a midline phenotype

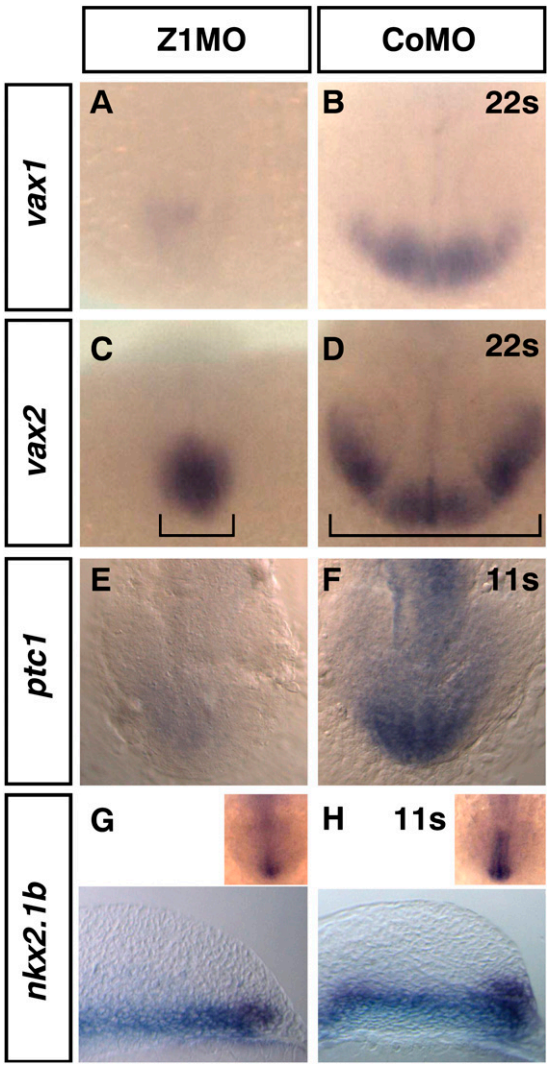

Figure 2. Zic1 morphants show reduced expression of Shh target genes. (*A–F*) Dorsal view, rostral to the *bottom*. (*A,B*) 22s. *Vax1* expression is strongly reduced in Zic1 morphants. (*C,D*) 22s. *Vax2* expression in the ventral retina of Zic1 morphants is down-regulated. Brackets indicate reduced proximal-distal *vax2* expansion. (*E,F*) 11s. *Ptc1*, a target gene of Shh, shows reduced expression. (*G,H*) Sagittal section, anterior to the *right*. The *inset* shows dorsal view, rostral to the *bottom*. 11s. *Nkx2.1b* expression in prospective hypothalamus is reduced in Zic1 morphants. (s) Somite stage.

can be observed as well, we investigated the expression of marker genes known to be downstream from Hedgehog signaling. *Patched1* (*ptc1*) is expressed in the ventral neuroectoderm of the brain (Concordet et al. 1996) and is known to be a target gene of Sonic hedgehog (Lewis et al. 1999). Z1MO-injected embryos show a clear reduction of *ptc1* expression (Fig. 2E). *Nkx2.1b*, which is expressed at early somitogenesis stages in the prospective hypothalamus (Rohr et al. 2001), shows a comparable reduction of expression (Fig. 2G). *Nkx2.1b* is also known to act downstream from the Hedgehog pathway (Rohr et al. 2001).

Zic1 interfers with Shh signaling by controlling shh *transcription*

The results above suggest that the expression of *sonic hedgehog* (*shh*) itself might be affected in Z1MO embryos. Indeed, injection of Z1MO into zebrafish embryos results in highly restricted loss of *shh* expression (Fig. 3; Supplemental Table S1). *Shh* expression in the anterior ventral diencephalon is absent from this domain from the onset of endogenous *shh* expression at the one- to two-somite stage, showing that *shh* expression in the anterior ventral diencephalon of Zic1 morphants is not initiated at all. *Shh* expression is undisturbed in domains showing no *zic1* expression, such as the underlying prechordal mesoderm, the notochord, and the floor plate of the spinal cord. The hedgehog homolog *twhh* shows a comparable reduction in expression in the ventral diencephalon (Fig. 3E).

If Zic1 controls the expression of *shh*, it should be possible to rescue the expression of Shh target genes like *ptc1* in Zic1 morphants by activating the Hedgehog pathway. Coinjection of Z1MO with *shh* mRNA resulted in a massive expansion of *ptc1* expression in neural tissue, suggesting that *shh* acts downstream from Zic1 (Fig. 4A; Supplemental Fig. S6A). Phenotypic rescue of Zic1 morphants could not be investigated, as overexpression of Shh affects morphogenesis (Ekker et al. 1995; Takamiya and Campos-Ortega 2006) and prevents rescue on a morphological level. Interestingly, however, coinjection of *shh* mRNA rescues apoptosis in optic vesicle and diencephalon (Supplemental Fig. S4C), demonstrating again that apoptosis is a secondary effect due to aberrant signaling earlier during forebrain development.

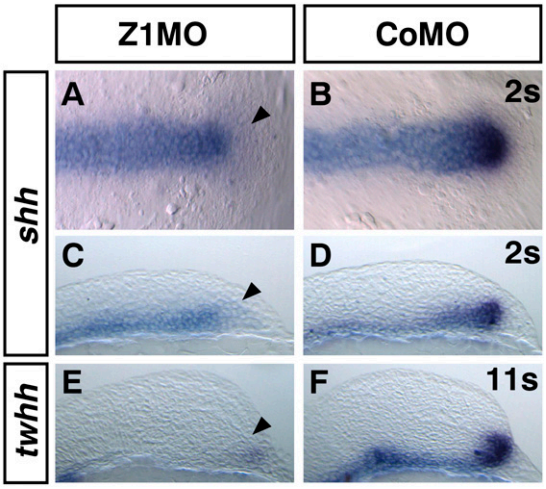

Figure 3. Zic1 morphants show specifically reduced *shh* and *twhh* expression. (*A,B*) Dorsal view of early forebrain, two-somite stage, rostral to the *right*. *Shh* expression is specifically reduced in ventral anterior diencephalon (black arrowhead). (*C,D*) Sagittal section, rostral to the *right*, 2s. (*E,F*) Sagittal section, rostral to the *right*. 11s. *Twhh* expression is strongly reduced in the ventral diencephalon (black arrowhead) of Zic1 morphants. (s) Somite stage.

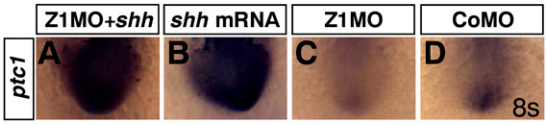

Figure 4. Zic1 knockdown does not interfere with *ptc1* induction by Shh overexpression. (*A–D*) Dorsal view, rostral to the *bottom*, 8s. (*A*) Simultaneous Zic1 knockdown and *shh* mRNA overexpression cannot block induction of the Shh target gene *ptc1*. (*B*) *Ptc1* induction by *shh* mRNA overexpression. (*C*) Z1MO injection leads to loss of *ptc1* expression in anterior forebrain tissue. (*D*) *Ptc1* wild-type expression in CoMO-injected embryos. (s) Somite stage.

Zic1 controls cyclops *expression and Nodal signaling in the ventral diencephalon*

Mice lacking Shh display cyclopia (Chiang et al. 1996). Zebrafish mutants defective for Hedgehog signaling, however, display only a relatively mild form of cyclopia (Barresi et al. 2000). Observation of severe midline defects in Zic1 morphants hence raises the possibility that loss of *shh* expression may not be the only cause of midline defects in Zic1 morphants. *Shh* expression in the ventral diencephalon is downstream from the Nodal pathway, and loss of Nodal signaling leads to loss of *shh* (and *twhh*) expression (Müller et al. 2000) and full cyclopia (Schier et al. 1997). As Zic1 is required for *shh* expression, we wondered if Zic1 is placed in between Shh and Nodal signaling or even upstream of Nodal signaling. To gain evidence for epistatic relation between Nodal signaling and Zic1, we tried to rescue *shh* expression in Zic1 morphants by activating the Nodal pathway through coinjection of a constitutively active construct of the Nodal signaling mediator smad2 (*smad2CA*) (Müller et al. 2000). Strikingly, coinjection of *smad2CA* mRNA and Z1MO leads to a clear up-regulation of *shh* expression above endogenous levels as opposed to down-regulation of *shh* expression in Zic1 morphants (Fig. 5A; Supplemental Fig. S6C). Thus, Zic1 does not appear to be required downstream from Nodal. Rescue on a morphological level could not be observed, as ectopic Nodal signaling by smad2CA overexpression affects embryological morphology (Müller et al. 2000). We next checked the expression of *cyclops* (*cyc*, *ndr2*), a Nodal ligand expressed in prechordal plate, axial mesoderm, and ventral forebrain (Rebagliati et al. 1998a; Sampath et al. 1998). We tested *cyc* expression in Zic1 morphants at the one-somite stage, when *cyc* shows expression in the anterior ventral forebrain (Rebagliati et al. 1998b). Interestingly, we observed a specific reduction of *cyc* expression exclusively in the ventral forebrain. *Cyc* expression in prechordal mesoderm and prechordal plate, however, remains unchanged (Fig. 5E; Supplemental Table S1). This is very reminiscent of the specific reduction of *shh* expression in Zic1 morphants. We used the Nodal-responsive *luciferase* reporter construct $(n2)_7$ Luc (Saijoh et al. 2000), to test if down-regulation of *cyc* results also in quantitative reduction of Nodal signaling. Coinjection of Z1MO with the Nodal reporter plasmid strongly reduced Nodal reporter activity compared with the control experiment (Fig. 5G), providing further strong evidence for reduced levels of Nodal signaling in the forebrain of Z1MO-injected embryos.

Zic1 morphants display a ventralized optic vesicle

Hedgehog signaling is known to promote ventral fate in the forebrain (Ekker et al. 1995; Macdonald et al. 1995; Lupo et al. 2005). Therefore, we expected that loss of Zic1 and ensuing loss of *shh* expression in the ventral

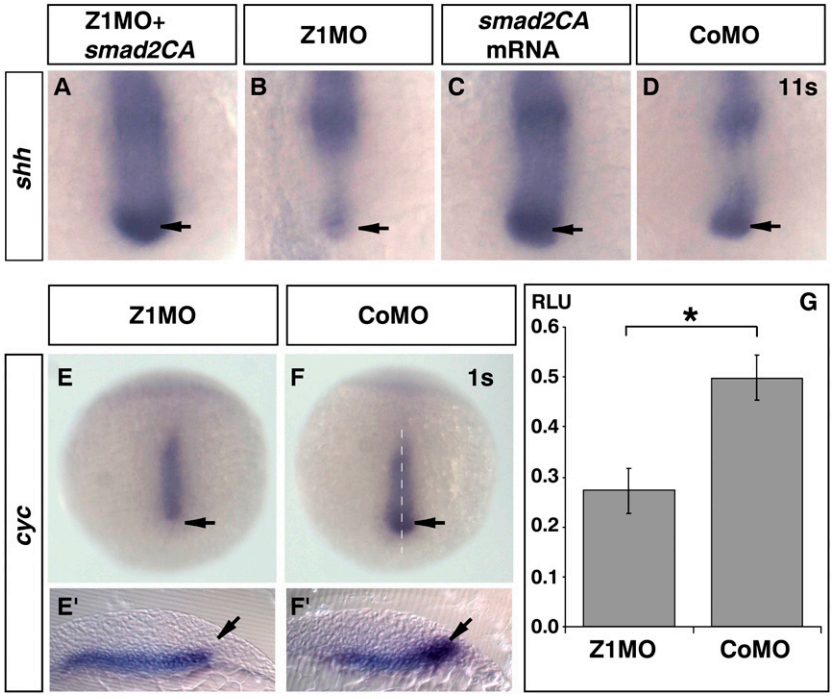

Figure 5. Zic1 controls *cyclops* expression and interferes with Nodal signaling. (*A–F*) Dorsal view, rostral to the *bottom*. (*A–D*) 11s. (*E–F′*) 1s. (*A*) Knockdown of Zic1 cannot block *smad2CA* mRNA-induced *shh* expression (arrow). (*B*) In Zic1 morphants, *shh* is down-regulated in the anterior forebrain (arrow). (*C*) *Smad2CA* mRNA injection causes induction of *shh* expression (arrow). (*D*) *Shh* expression in the anterior forebrain of CoMO-injected embryos (arrow). (*E–F′*) *Cyc* expression is strongly down-regulated in the anterior ventral forebrain of Zic1 morphants (arrow; dashed line indicates level of sections). (*G*) A Nodal luciferase reporter construct indicates reduced Nodal signaling in Zic1 morphants at the 1–2-somite stage. Error bars indicate SEM. Asterisk indicates statistical significance; *t*-test, (*) $p < 0.05$. (RLU) Normalized relative light units; (s) somite stage.

diencephalon would be accompanied by an expansion of markers of the dorsal optic vesicle. We thus investigated the expression of marker genes for dorsal–ventral patterning of the optic vesicle by WMISH to confirm this.

Surprisingly, Zic1 morphants show the opposite phenotype: Dorsal marker genes like *pax6*, the BMP target *tbx5* (Begemann and Ingham 2000), and the BMP activator *radar* (Rissi et al. 1995) get down-regulated; the ventral expression domain of *pax2* in the prospective optic stalk, however, expands up to the dorsalmost region of the optic vesicle (Fig. 6; Supplemental Table S1). This was especially surprising, as embryos with reduced Hedgehog signaling always show reduced *pax2* expression. (Ekker et al. 1995; Macdonald et al. 1995; Lupo et al. 2005).

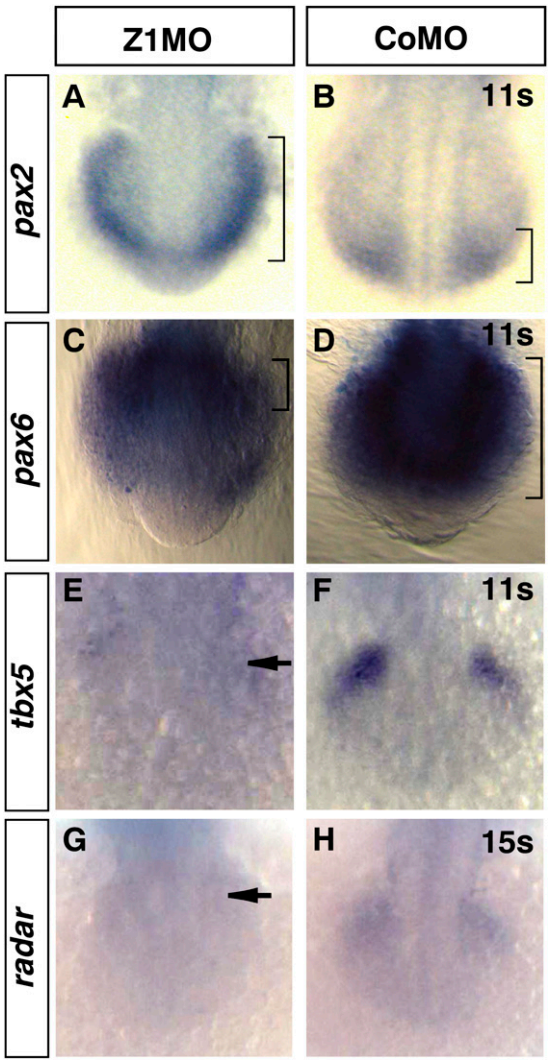

Figure 6. Zic1 morphants display a ventralized optic vesicle. (*A–H*) Dorsal view, rostral/ventral to the *bottom*, 11s–15s. (*A–B*) Zic1 morphants show ectopic *pax2* expression in prospective retinal tissue (brackets indicate dorsal expansion). (*C,D*) *Pax6* retinal expression, in contrast, retracts to most dorsal retinal domains (brackets indicate retraction of *pax6* expression). (*E,F*) *Tbx5* expression in the dorsal retina is strongly reduced (arrow). (*G,H*) *Radar* expression in the dorsal retina is strongly reduced (arrow). (s) Somite stage.

As dorsal–ventral patterning of the optic vesicle is under control of several pathways (Lupo et al. 2006), we reasoned that besides loss of *shh* expression, another signaling pathway promoting ventral fate during optic vesicle development might get overactivated in Zic1 morphants. Notably, FGF and RA signaling are known to promote ventral fate in the optic vesicle (Lupo et al. 2005). First, we investigated whether *fgf3* or *fgf8*, two FGF genes that play a key role during early zebrafish forebrain and optic stalk development (Walshe and Mason 2003), show any change in expression. Both *fgf3* and *fgf8* show strongly reduced expression in the forebrain of Zic1 morphants at the tailbud and early somite stage, providing evidence against increased FGF signaling in the early forebrain (Supplemental Fig. S7; Supplemental Table S1).

Zic1 LOF up-regulates RA signaling in the forebrain

Next, we checked for aberrant RA signaling. Spatio-temporal levels of RA signaling in the zebrafish forebrain during gastrulation and neurulation are controlled by the anteriorly expressed RA-degrading enzyme Cyp26a1 and the posteriorly expressed RA-generating enzyme Raldh2 (Hernandez et al. 2007; White et al. 2007). *Raldh2* is never coexpressed with *zic1* and shows no change in expression levels after Z1MO injection (data not shown). *Cyp26a1*, however, is coexpressed with *zic1* in the forebrain region during zebrafish gastrulation and the tailbud stage (cf. also Fig 7B and Supplemental Fig S1A; Kudoh et al. 2002; Hernandez et al. 2007). Strikingly, injection of Z1MO leads to down-regulation of *cyp26a1* expression specifically in the forebrain region (Fig. 7A; Supplemental Table S1), the region where *zic1* and *cyp26a1* are coexpressed. Down-regulation of *cyp26a1* expression should therefore result in lower RA degradation rates and hence elevated RA signaling. To investigate this, we injected embryos transgenic for a RA-sensitive GFP reporter (Perz-Edwards et al. 2001) with Z1MO. Z1MO-injected embryos show a massive up-regulation of RA reporter activity in anterior neural tissue at the 18-somite stage, indicating a strong increase in RA signaling in anterior neural tissue (Fig. 7C–D′). Furthermore, coinjection of a *luciferase* reporter gene under control of RA-responsive RARE elements (Blumberg et al. 1997) together with Z1MO into zebrafish embryos indicate increased activation of the RA reporter gene (data not shown), further proving that RA signaling in the forebrain is elevated.

If the optic vesicle in Zic1 morphants is ventralized because of enhanced RA signaling, it should be possible to revert ventralization by blocking RA signaling. As predicted, incubation of Z1MO-injected embryos with the RA signaling inhibitor DEAB reduced the expanded expression of *pax2* back to ventral domains of the optic vesicle (Fig. 7E–H; Supplemental Fig. S6B).

We therefore conclude that Zic1 is required for maintenance of expression of the RA-degrading enzyme Cyp26a1 in the forebrain and that interfering with Zic1 function results in reduced *cyp26a1* expression and hence elevated levels of RA signaling in the forebrain leading to ventralization of the optic vesicle.

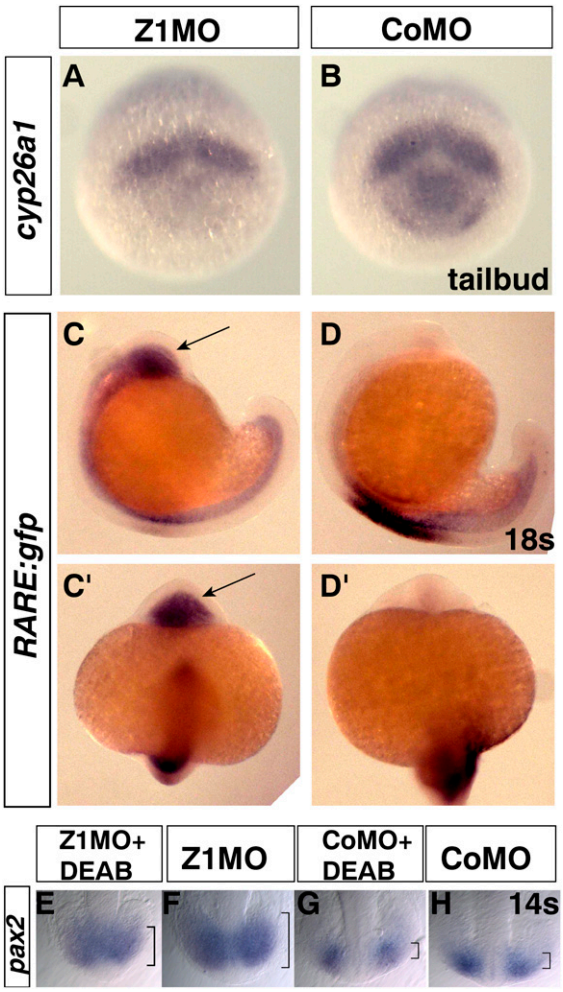

Figure 7. Zic1 LOF up-regulates RA signaling in the forebrain. (*A*,*B*) Tailbud stage, rostral view, dorsal to the *top*. *Cyp26a1* expression is strongly reduced in prospective forebrain tissue of Zic1 morphants. (*C*,*D*) Lateral view, 18s, anterior to the *right*. Injection of Z1MO into embryos transgenic for a RA-sensitive gfp reporter leads to a massive up-regulation of reporter activity in anterior neural tissue (arrow) (n = 52, 90%) as compared with control (n = 31). (*C*′–*D*′) Anterior view, 18s. Arrow indicates up-regulated reporter expression. Detection of *gfp* by WMISH due to low signal intensity of the Gfp fluorescence. (*E*–*H*) Dorsally expanded *pax2* expression in the optic vesicle of Zic1 morphants can be rescued by administration of the RA inhibitor DEAB (brackets indicate dorsal expansion). (*G*) *Pax2* expression in control embryos treated with DEAB is slightly weaker than in controls. (*H*) *Pax2* expression in control embryos. (s) Somite stage.

Differential rescue of forebrain marker genes in Zic1 morphants by overexpression of cyp26a1 *and* shh *mRNA*

Initial rescue experiments with *shh* mRNA and the RA signaling inhibitor DEAB suggested that the patterning defects in Zic1 morphants are caused by down-regulation of Hedgehog and up-regulation of RA signaling. We thus tried to rescue both signaling events by the simultaneous overexpression of *shh* and *cyp26a1* mRNA. We followed four key marker genes (*vax1*, *vax2*, *pax2*, and *pax6*) comparing the single- and the double-pathway rescue.

The expression of the optic stalk marker *vax1* in Zic1 morphants can be rescued by *shh* mRNA overexpression, confirming that loss of *vax* gene expression is caused by reduced Hedgehog signaling. Simultaneous overexpression of *cyp 26a1* and *shh* mRNA results in a similar rescue of *vax1* as with *shh* mRNA only (Fig. 8A–E; Supplemental Table 2). Reduced *vax2* expression in Zic1 morphants is also rescued by *shh* at least in proximal optic stalk domains. The rescue of distal retinal *vax2* expression by Shh is weaker. Attenuation of RA signaling through *cyp26a1* overexpression or simultaneous *cyp26a1*/*shh* mRNA overexpression reduces the diminished *vax2* expression domain in Zic1 morphants to an even smaller proximal domain (Fig. 8F–J). This indicates that the remaining proximal *vax2* expression domain in Zic1 morphants is maintained by increased RA levels in an otherwise Hedgehog-deprived Zic1 morphant environment and that up-regulation of *vax2* by *shh* is at least partially RA-dependent. Expansion of *pax2* expression into retinal domains of Zic1 morphants can be rescued by *cyp26a1* overexpression. This confirms again that expansion of *pax2* expression is indeed elicited by elevated RA signaling levels. *Shh* mRNA co-overexpression can override this rescue, indicating that ectopic *pax2* expression induced by *shh* mRNA is not RA-dependent, unlike *vax2* expression (Fig. 8K–O). Reduced *pax6* expression in Zic1 morphants is rescued by *cyp26a1* overexpression, confirming that ventralization of the retina is elicited by elevated RA signaling. As expected, overexpression of *shh* mRNA in Zic1 morphants reduces *pax6* expression even further. Co-overexpression of *cyp26a1* with *shh* in Zic1 morphants attenuates this extreme reduction of *pax6* expression (Fig. 8P–T).

As elevated RA signaling could be also responsible for down-regulation of *cyc* and *shh*, we also tried to rescue these two genes by *cyp26a1* overexpression. However, no rescue can be detected (Fig. 8U–Z). An independent rescue experiment for *cyc* yielded the same result (Supplemental Fig. S6D). In summary, *shh* overexpression can rescue ventral marker genes dependent on Hedgehog signaling, and *cyp26a1* overexpression reduces artificially high RA levels, therewith reverting forced ventralization of the optic vesicle in Zic1 morphants. It may not be reasonable to suspect that we could find exactly the correct protocol, using the misexpression techniques we have, to rescue the entire Zic1 morphant phenotype by overexpression of these two signaling molecules because both increased RA and increased *shh* signaling are known to affect morphogenesis of the optic vesicle (Hyatt et al. 1992; Macdonald et al. 1995).

Discussion

Zic1 knockdown causes defective forebrain midline development and ventralization of the optic vesicle at the same time

In this study, we demonstrate that knockdown of Zic1 in zebrafish elicits a strong midline defect. The observed

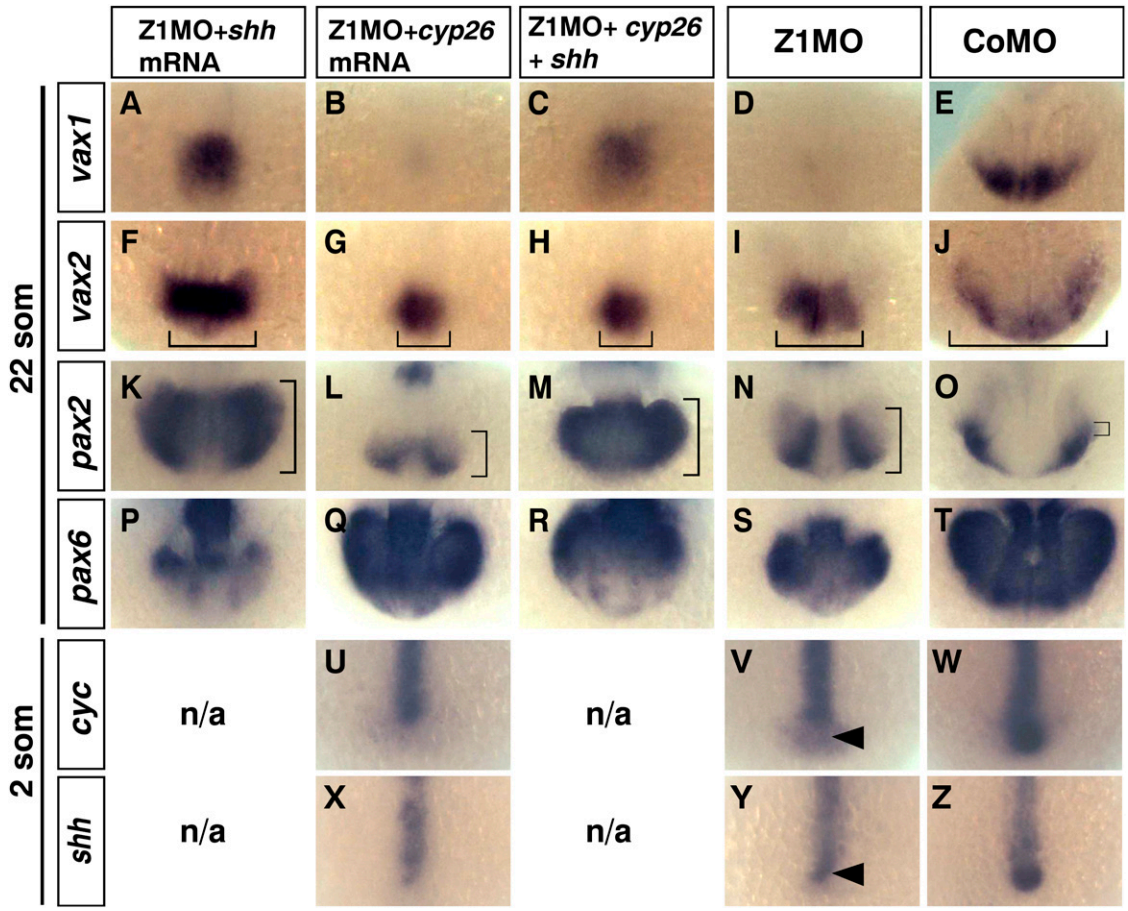

Figure 8. Differential rescue of marker genes in Zic1 morphants by overexpression of *cyp26a1* and *shh* mRNA. (*A–Z*) Forebrain region, dorsal view, rostral to the *bottom*. (*A–T*) 22-somite stage; (*U–Z*) Two-somite stage. (*A–E*) Abolished *vax1* expression in Zic1 morphants can be rescued by overexpression of *shh* mRNA. *Cyp26a1* mRNA overexpression in Zic1 morphants does not rescue *vax1* expression. Simultaneous overexpression of *shh* and *cyp26a1* leads to a similar rescue as with *shh* only. (*F–J*) Reduced *vax2* expression in Zic1 morphants can be rescued to some extent by *shh* overexpression. *Cyp26a1* overexpression in Zic1 morphants causes a further reduction of *vax2* expression, however. Simultaneous overexpression of *shh* and *cyp26a1* in Zic1 morphants results in a similar reduction of *vax2* expression as with *cyp26a1* only. Brackets indicate proximal-distal expansion. (*K–O*) Overexpression of *cyp26a1* rescues dorsal expansion of *pax2* in Zic1 morphants. Dorsal expansion of *pax2* expression in the prospective retina of Zic1 morphants is promoted by *shh* overexpression. Simultaneous overexpression of *shh* and *cyp26a1* leads to similar expansion as with *shh* only. Brackets indicate ventral–dorsal expansion. (*P–T*) Overexpression of *cyp26a1* in Zic1 morphants leads to a rescue of dorsal *pax6* retraction. Dorsally retracted *pax6* expression in Zic1 morphants is exacerbated by *shh* overexpression. *Pax6* expression after simultaneous overexpression of *shh* and *cyp26a1* in Zic1 morphants resembles *pax6* expression in Zic1 morphants. (*U–Z*) Reduced *cyc* and *shh* expression in Zic1 morphants (arrowhead) cannot be rescued by *cyp26a1* overexpression. (som) Somite stage; (n/a) not applicable.

features, such as fusion of RPE, partial cyclopia, and conversion of optic stalk into pigmented tissue, indicate aberrant development of midline structures. Other features of Zic1 morphants, however, indicate that not just midline formation is impaired: A severe midline phenotype in Zic1 morphants is always accompanied by a strong reduction of ventral RPE. Reduction of ventral RPE, however, can be frequently observed in embryos with elevated signaling levels of ventralizing pathways, like Shh (Macdonald et al. 1995). Neural midline defects, in contrast, are usually caused by attenuated ventralizing signals like Shh; therefore, these two features of the phenotype seem to contradict each other. An analysis of marker gene expression during earlier stages confirms this complex phenotype: On the one hand, *shh* expression in the anterior ventral diencephalon is down-regulated and, as expected, this results in reduced expression of Shh target genes (*ptc1*, *nkx2.1b*, *vax1*, and *vax2*) promoting midline development. On the other hand, marker genes for dorsal–ventral patterning of the optic vesicle indicate strong ventralization of the optic vesicle in Zic1 morphants. The dorsal retraction of RPE is the consequence of the ventralization. However, this is exactly the opposite phenotype expected in embryos with abolished *shh* forebrain expression (Ekker et al. 1995; Macdonald et al. 1995).

Increased RA signaling in the forebrain of Zic1 morphants is the reason for ventralization of the optic cup

It is clear that loss of *shh* expression cannot be the sole reason for the disarray of forebrain patterning. Examination of FGF and RA signaling levels showed that in Zic1 morphants, early FGF signaling in the forebrain is massively reduced as well, but RA signaling proved to be up-regulated. The up-regulation of RA signaling allows a coherent interpretation of the ventralization phenotype. Whereas Shh and its target genes become down-regulated, elevated RA signaling exerts a ventralizing effect on optic vesicle and marker genes *pax6*, *pax2*, *tbx5*, and *radar*. Interestingly, RA seems to be able to expand expression of the optic stalk marker *pax2* in Zic1 morphants independently of Hedgehog and FGF signaling, whereas this seems not to be the case with other optic stalk markers like *vax1* and *vax2*. It has been shown before that increased RA signaling in zebrafish results in expansion of *pax2* expression into the optic vesicle (Hyatt et al. 1996) and repression of *tbx5* expression (Emoto et al. 2005).

Could increased RA signaling in the forebrain also be the reason why *shh* expression is repressed? Studies performed in *Xenopus* (Franco et al. 1999; Lupo et al. 2005) demonstrate that high doses of RA (1–10 μM) repress anterior *shh* expression in the forebrain. However, our rescue experiments with coinjected *cyp26a1* mRNA were not successful in restoring *shh* or *cyc* expression in the forebrain. This might be due to experimental limitations, as strong up-regulation or down-regulation of RA signaling during early development causes gastrulation defects, which limits the amount of injected *cyp26a1* mRNA or other reagents modulating RA signaling. Failed rescue experiments might thus reflect the difficulties of modulating RA levels in anterior neuroectoderm only. However, studies of *cyp26a1* knockout mice and *cyp26a1* zebrafish mutants do not report any forebrain midline defects, arguing against regulation of Hedgehog or Nodal expression endogenously by *cyp26a1* only (Abu-Abed et al. 2001; Emoto et al. 2005).

Increased RA levels may contribute to defective dorsal midline development. BMP signaling is necessary for dorsal midline development in the mammalian forebrain (Fernandes et al. 2007). Our results show that expression of genes playing a role upstream of or downstream from BMP signaling like *radar* and *tbx5* are down-regulated in the zebrafish by increased RA levels. The ectopic up-regulation of RA signaling in the dorsal forebrain in Zic1 morphants could thus explain why *zic2* mutations in mammals are associated with MIH HPE as well (Fernandes and Hébert 2008). In this context, it is useful to note that the late up-regulation of *fgf8* expression that we see in the telencephalon at 26 hpf has also been described after ectopic activation of RA signaling in the zebrafish (Hamade et al. 2006). That study is particularly interesting because RA treatment (starting at 75% epiboly until the 10-somite stage) coincides with the onset of Zic1 expression and roughly with the time window when we observed regulation of respective marker genes. Studies in mouse and chick have also shown dependency of *fgf8* forebrain expression on RA signaling (Schneider et al. 2001; Maden et al. 2007).

Attenuated Nodal signaling in Zic1 morphants is the reason for severe midline defects and reduced shh *expression*

Severity of the Zic1 morphant midline phenotype and reduced *shh* expression indicate that Nodal signaling upstream of *shh* might be impaired, as loss of Nodal midline signaling in zebrafish results in most severe midline defects including full cyclopia (Schier et al. 1997) and abolished *shh* expression (Müller et al. 2000; Rohr et al. 2001). Our observations confirm this hypothesis, showing that *cyc* expression in the anterior ventral forebrain of Zic1 morphants is down-regulated, that Nodal signaling levels are reduced, and that coexpression of Smad2, a Nodal signaling mediator, rescues *shh* expression in the forebrain. In Zic1 morphants, loss of *cyc* and *shh* expression is restricted to the anterior ventral forebrain. *cyc* and *shh* expression domains in axial mesodermal tissue do not show significant change. As Zic1 morphants do not show full cyclopia like Nodal signaling mutants, residual Nodal/Hedgehog signaling from axial mesoderm might still confer some midline signaling activity to the ventral forebrain.

Interestingly, early expression of *fgf* genes at the tailbud stage is reduced as well. This is of relevance as Nodal, Hedgehog, and FGF signaling have been shown to positively regulate each other during early development in

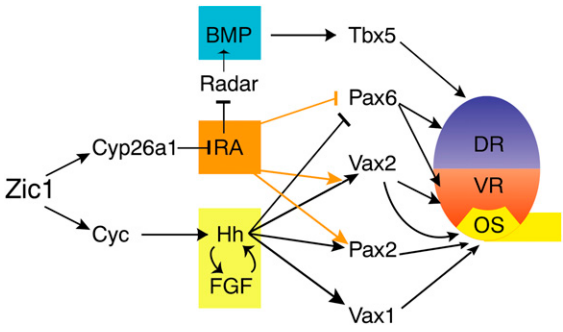

Figure 9. Network model summarizing observed regulation events. Zic1 controls expression of *cyc* and *cyp26a1*. *Cyc* controls *shh*, which regulates transcription of its target genes *vax1* (optic stalk), *pax2* (optic stalk), and *vax2* (optic stalk, ventral retina). *Cyp26a1* maintains RA signaling at low levels during early forebrain development. In Zic1 morphants, *cyp26a1* and *cyc* expression is down-regulated. Nodal, Hedgehog, and FGF signaling is hence reduced in the forebrain, and RA signaling is increased. *Vax1* expression is lost. Elevated RA signaling expands the *pax2* expression domain independently of Hedgehog signaling into the retina. *Vax2* expression is reduced to a most proximal domain, as elevated RA signaling cannot compensate reduced Hedgehog signaling. *Pax6*, *tbx5*, and *radar* expression is repressed due to elevated RA signaling. (DR) Dorsal retina; (VR) ventral retina; (OS) optic stalk.

signaling cross-talk events (Mathieu et al. 2002, 2004; Walshe and Mason 2003). Thus, reduced FGF signaling at the tailbud stage in the early anterior forebrain of Zic1 morphants might cause a breakdown of the Nodal/Hedgehog/FGF signaling cross-talk leading to loss of *cyc* and *shh* expression during early somite stages.

Zic1 regulates Nodal, Hedgehog, and RA signaling in the forebrain

In summary, we are proposing a model in which Zic1 controls activity of the Nodal, Hedgehog, and RA signaling pathways in the forebrain (Fig. 9). Zic1 maintains *cyp26a1* expression in the forebrain from the 70% epiboly to the tailbud stage. This ensures that RA signaling levels are low in the forebrain and optic vesicle. At the one- to two-somite stage, Zic1 is required for onset of *cyc* expression in the anterior ventral diencephalon. *cyc* expression in turn controls *shh* expression and therefore expression of Shh target genes and *fgf* genes.

If Zic1 function is abolished, *cyp26a1* expression in the forebrain is strongly reduced, leading to elevated levels of RA signaling and subsequent ventralization of the optic vesicle. Concomitantly, *pax2* expression expands into the retina, and *pax6*, *tbx5*, and *radar* expression is repressed. In the anterior ventral forebrain of Zic1 morphants, *cyc* expression cannot be induced. This causes loss of *shh* expression and consequently reduced expression of the Shh target genes: *vax1*, *vax2*, *nkx2.1b*, and *ptc1*.

Loss of Zic1 in zebrafish as a model to dissect molecular pathways causing different forms of HPE in humans and mouse

Our data suggest that Zic1 is the main Zic factor controlling zebrafish midline signaling, in contrast to mammalian development, where Zic2 is required for midline development. The closest zebrafish homolog of Zic2—Zic2a—has been shown in this study to act in a more redundant way. It would be interesting, therefore, to see if a double knockout of mouse Zic1 and Zic2 would yield an even stronger midline defect than reported in Zic2 mutants. Aruga et al. (2002a) tried to obtain Zic1/Zic2 double-homozygous mice but did not succeed because of the poor health of mice heterozygous for both Zic1 and Zic2. Perhaps Zic1/Zic2 double-heterozygous mice at early developmental stages might tell us whether RA, Nodal, and Shh signaling are controlled in mammals in the same way as has been demonstrated in this study for zebrafish.

Our results provide possible insights into a variety of hitherto unexplained effects observed in Zic mouse mutants, such as neurulation defects in the forebrain (Nagai et al. 2000) and aberrant inhibition of neurogenesis (Brewster et al. 1998; Aruga et al. 2002b) as these might be elicited by elevated RA signaling (Franco et al. 1999; Abu-Abed et al. 2001). More strikingly, however, the data in this study provide a unifying molecular explanation of why loss of Zic function can cause both classic HPE as well as MIH HPE.

Materials and methods

Fish strains

Embryos were obtained from natural spawnings of wild-type zebrafish lines (TL, *Danio rerio*). Embryos were raised at 28.5°C and staged according to Kimmel et al. (1995).

Subcloning Zic1 in pCS2+

The *D. rerio* Zic1 ORF was PCR-amplified from Zic1-pSport (Rohr et al. 1999) and subcloned into pCS2+ by EcoRI/XhoI to allow in vitro mRNA synthesis.

RNA microinjection

Synthetic mRNA was transcribed using the Ambion mMessage mMachine in vitro transcription kit. mRNA was injected at the one-cell stage. Synthetic mRNAs were injected at the following concentrations: 80–120 pg of *Zic1* (Rohr et al. 1999), 80–120 pg of *gfp*, 30–60 pg of *shh* (Macdonald et al. 1995), 100 pg of *bcl2gfp* (Langenau et al. 2005), 5 pg of *smad2CA* (Müller et al. 2000), and 120 pg of *cyp26a1* (Gongal and Waskiewicz 2008).

Morpholinos

Morpholinos were obtained from GeneTools. Morpholinos were dissolved in water and injected at the one-cell stage. CoMO is the GeneTools standard control morpholino. The Zic1 morpholino was designed to target the *zic1* exon 1–intron 1 boundary (Z1MO; 5′-ATAACGATTTTCTTACCTGTGTGTG-3′). The Z2aMO sequence is 5′-CTCTTTCAAGCAGTCTATTCACGGC-3′ (Sanek and Grinblat 2008).

Z1MO is designed to block splicing at the exon 1–intron 1 boundary of the *zic1* transcript. Analysis of the splice blocking event reveals that injection of Z1MO into zebrafish embryos blocks excision of intron 1 and leads to inclusion of 60 base pairs of intron 1 containing a stop codon, prematurely terminating the protein coding sequence (Supplemental Fig. S3). This results in loss of the C-terminal part of the protein including the two C-terminal zinc fingers. Injection of a Zic1 translation blocking morpholino resulted in a phenotype similar to the Z1MO phenotype, confirming that Z1MO leads to complete LOF of Zic1 (data not shown).

Efficacy and specificity of the splice inhibitor morpholino (Z1MO) were controlled by RT–PCR at different stages (tailbud, five-somite, 17-somite). Three nanograms to 4 ng of Z1MO was injected per embryo.

Monitoring efficacy

Inhibition of splicing of the *zic1* transcript should lead to inclusion of intron1 (or part of it) in the mature *zic1* mRNA (Supplemental Fig. S3A). This was expected to result in a bandshift of the RT–PCR-amplified *zic1* fragment, as RT–PCR primers (Zic1 Ex1 → Ex3 L + R) are located upstream of and downstream from intron 1 in exons 1 and 3, respectively. Z1MO injection resulted in a complete bandshift of the amplified fragment, mirroring the inclusion of 60 bases of intron 1 in virtually all endogenous *zic1* mRNAs. As the included 60 bases contain an in-frame stop codon, truncation of the Zic1 protein results (Supplemental Fig. S3C).

Specificity was monitored by taking advantage of sequence conservation among *zic* genes. The Z1MO targeted sequence at the *zic1* exon 1–intron 1 boundary differs only in seven out of 25 bases from the *zic2a* exon 1–intron 1 boundary and in

10 out of 25 from the *zic2b* exon 1–intron 1 boundary. Monitoring of aberrant splicing of endogenous *zic2a* or *zic2b* mRNA transcripts would indicate that Z1MO would inhibit splicing off-target. No nonspecific splicing was observed, however (Supplemental Fig. S3B).

Pharmacological treatment

DEAB (diethylaminobenzaldehyde; kind gift of Kate Lewis) was stored as a 100 mM stock solution in DMSO at −20°C. At the one-cell stage, injected embryos were placed at the germring stage in chorions in embryo medium containing 30 μM DEAB and raised at 28.5°C in the dark. Sibling control embryos were incubated in embryo medium containing corresponding DMSO concentrations. Embryos were fixed in 4%PFA/PBS at the 14- to 17-somite stage.

Luciferase assays

Embryos used for Luciferase assays were coinjected with premixed reporter plasmid and Renilla control plasmid to allow normalization. Embryos were injected at the one-cell stage. The injected DNA amounts were 12 pg of RA *luciferase* reporter tk-$(\beta RARE)_2$-luc (Blumberg et al. 1997), 10 pg of Nodal *luciferase* reporter $(n2)_7$ Luc (Saijoh et al. 2000), and 5 pg of Renilla control *luciferase* reporter (Promega). Thirty to 50 embryos per condition were transferred at appropriate developmental stage into 1 mL of Passive Lysis Buffer (Promega) and homogenized by passing embryos six to seven times through a G20 needle. Detection was carried out according to manufacturers' recommendations (Dual-Luciferase Reporter Assay System, Cat. no. E1910; Promega) on a Turner Designs TD-20/20 Luminometer.

RT–PCR

Embryos used for RT–PCR were homogenized by passing 10 to 20 embryos in 300 μL of RLT kit buffer through a G20 needle three to four times. RNA isolation was accomplished according to manufacturers' recommendations (Qiagen MicroRNA isolation kit). Subsequent RT–PCR was performed according to manufacturers' recommendations (Qiagen OneStep RT–PCR kit). We used the RT–PCR program as follows: 30 min at 50°C, 15 min at 95°C, 35 times (30 sec at 94°C, 30 sec at 60°C, 2 min at 72°C), and 1 min at 72°C.

The RT–PCR primers were Zic1 Ex1 → 3_L, 5′-CCGATCGG AAAATCTGAAAA-3′; Zic1 Ex1 → 3_R, 5′-TCGTGTGGTGA ACTGTGGAT-3′; Zic1 Ex1_L, 5′-CATCACCCCACTCATG TCAG-3′; Zic1 Ex1_R, 5′-CAGGCGCATCTGACTGTTTA-3′; Zic2a Ex1 → 3_L, 5′-CTCGCTCCATCATTCTCACA-3′; Zic2a Ex1 → 3_R, 5′-GGAGGGAGACACCAGACCA-3′; Zic2a Ex1_L, 5′-CTCGCTCCATCATTCTCACA-3′; Zic2a Ex1_R, 5′-CTTAA TGCACTGCTGCCTCA-3′; Zic2b Ex1 → 3_L, 5′-GGATTACC CGGTGAGGTTTT-3′; Zic2b Ex1 → 3_R, 5′-TTAAACGTACC ACTCGTTA-3′; Zic2b Ex1_L, 5′-GGATTACCCGGTGAGGT TTT-3′; Zic2b Ex1_R, 5′-TGGTGCTGAAAGTTTTGCTG-3′; β-actin_L, 5′-CATCAGCATGGCTTCTGCTCT-3′; β-actin_R, 5′-GCAGTGTACAGAGACACCC-3′.

WMISH and whole-mount immunohistochemistry

Embryos were fixed in 4% paraformaldehyde/PBS. WMISH was carried out as described in Concordet et al. (1996) using the following probes: *zic1* (Rohr et al. 1999); *vax1, vax2* (Take-uchi et al. 2003); *fgf3* (Walshe and Mason 2003); *ptc1* (Concordet et al. 1996); *nkx2.1b* (Rohr et al. 2001); *shh* (Krauss et al. 1993); *cyclops* (Rebagliati et al. 1998a); *pax2* (Krauss et al. 1991a); *pax6* (Krauss et al. 1991b); *tbx5* (Begemann and Ingham 2000); *radar* (Rissi et al. 1995); *cyp26a1* (Kudoh et al. 2002; White et al. 2007); *fgf3* (Maves et al. 2002); *fgf8* (Shanmugalingam et al. 2000).

Active Caspase-3 was detected with a monoclonal rabbit antibody from BD Pharmingen (catalog no. 559565) at a dilution of 1:500. Primary antibody was visualized by an Alexa Fluor 488-coupled secondary donkey anti-rabbit antibody (1:400).

Sections

Vibratome sections were performed with a Vibratome Series 1000. Embryos were embedded in a BSA/gelatine mixture and sectioned at 20 μm.

Acknowledgments

We thank Guiseppe Lupo for discussions, helpful advice, plasmids, and morpholinos. We thank Julien Falk, Patricia Jussuf, and Caren Norden for discussions and help with the manuscript, and Katrina Holmes, Adrian McNabb, and Ashish Pungaliya for technical assistance. We thank Gaia Gestri, Claus Schulte, Gustavo Cerda-Moya, and Manuel Batista for help, plasmids, and reagents. We thank Kate Lewis for the kind gift of DEAB and plasmids, and Thomas Look, Ivor Mason, Igor Dawid, Uwe Strähle, Steve Wilson, Hiroshi Hamada, Bruce Blumberg, Lisa Maves, Andrew Waskiewicz, and Thomas Schilling for the kind gift of plasmids. We thank Steve Wilson for embryos of the RARE:YFP zebrafish line. This work was funded by a research fellowship from the Deutsche Forschungsgemeinschaft (DFG) and a program grant from the Wellcome Trust (to W.A.H.).

References

Abu-Abed S, Dollé P, Metzger D, Beckett B, Chambon P, Petkovich M. 2001. The retinoic acid-metabolizing enzyme, CYP26A1, is essential for normal hindbrain patterning, vertebral identity, and development of posterior structures. *Genes & Dev* **15:** 226–240.

Aruga J, Inoue T, Hoshino J, Mikoshiba K. 2002a. Zic2 controls cerebellar development in cooperation with Zic1. *J Neurosci* **22:** 218–225.

Aruga J, Tohmonda T, Homma S, Mikoshiba K. 2002b. Zic1 promotes the expansion of dorsal neural progenitors in spinal cord by inhibiting neuronal differentiation. *Dev Biol* **244:** 329–341.

Barresi MJ, Stickney HL, Devoto SH. 2000. The zebrafish slow-muscle-omitted gene product is required for Hedgehog signal transduction and the development of slow muscle identity. *Development* **127:** 2189–2199.

Begemann G, Ingham PW. 2000. Developmental regulation of Tbx5 in zebrafish embryogenesis. *Mech Dev* **90:** 299–304.

Bertrand N, Dahmane N. 2006. Sonic hedgehog signaling in forebrain development and its interactions with pathways that modify its effects. *Trends Cell Biol* **16:** 597–605.

Blumberg B, Bolado J Jr, Moreno TA, Kintner C, Evans RM, Papalopulu N. 1997. An essential role for retinoid signalling in anteroposterior neural patterning. *Development* **124:** 373–379.

Brewster R, Lee J, Ruiz i Altaba A. 1998. Gli/Zic factors pattern the neural plate by defining domains of cell differentiation. *Nature* **393:** 579–583.

Brown SA, Warburton D, Brown LY, Yu CY, Roeder ER, Stengel-Rutkowski S, Hennekam RC, Muenke M. 1998. Holoprosencephaly due to mutations in ZIC2, a homologue of *Drosophila* odd-paired. *Nat Genet* **20:** 180–183.

Brown LY, Odent S, David V, Blayau M, Dubourg C, Apacik C, Delgado MA, Hall BD, Reynolds JF, Sommer A, et al. 2001. Holoprosencephaly due to mutations in ZIC2: Alanine tract expansion mutations may be caused by parental somatic recombination. *Hum Mol Genet* **10:** 791–796.

Chiang C, Litingtung Y, Lee E, Young KE, Corden JL, Westphal H, Beachy PA. 1996. Cyclopia and defective axial patterning in mice lacking Sonic hedgehog gene function. *Nature* **383:** 407–413.

Cohen MM Jr. 2006. Holoprosencephaly: Clinical, anatomic, and molecular dimensions. *Birth Defects Res A Clin Mol Teratol* **76:** 658–673.

Concordet JP, Lewis KE, Moore JW, Goodrich LV, Johnson RL, Scott MP, Ingham PW. 1996. Spatial regulation of a zebrafish patched homologue reflects the roles of sonic hedgehog and protein kinase A in neural tube and somite patterning. *Development* **122:** 2835–2846.

Ekker SC, Ungar AR, Greenstein P, von Kessler DP, Porter JA, Moon RT, Beachy PA. 1995. Patterning activities of vertebrate hedgehog proteins in the developing eye and brain. *Curr Biol* **5:** 944–955.

Elsen GE, Choi LY, Millen KJ, Grinblat Y, Prince VE. 2008. Zic1 and Zic4 regulate zebrafish roof plate specification and hindbrain ventricle morphogenesis. *Dev Biol* **314:** 376–392.

Emoto Y, Wada H, Okamoto H, Kudo A, Imai Y. 2005. Retinoic acid-metabolizing enzyme Cyp26a1 is essential for determining territories of hindbrain and spinal cord in zebrafish. *Dev Biol* **278:** 415–427.

Fernandes M, Hébert JM. 2008. The ups and downs of holoprosencephaly: Dorsal versus ventral patterning forces. *Clin Genet* **73:** 413–423.

Fernandes M, Gutin G, Alcorn H, McConnell SK, Hébert JM. 2007. Mutations in the BMP pathway in mice support the existence of two molecular classes of holoprosencephaly. *Development* **134:** 3789–3794.

Franco PG, Paganelli AR, López SL, Carrasco AE. 1999. Functional association of retinoic acid and hedgehog signalling in *Xenopus* primary neurogenesis. *Development* **126:** 4257–4265.

Gongal PA, Waskiewicz AJ. 2008. Zebrafish model of holoprosencephaly demonstrates a key role for TGIF in regulating retinoic acid metabolism. *Human Mol Gen* **17:** 525–538.

Grinblat Y, Sive H. 2001. zic gene expression marks anteroposterior pattern in the presumptive neurectoderm of the zebrafish gastrula. *Dev Dyn* **222:** 688–693.

Grinblat Y, Gamse J, Patel M, Sive H. 1998. Determination of the zebrafish forebrain: Induction and patterning. *Development* **125:** 4403–4416.

Hamade A, Deries M, Begemann G, Bally-Cuif L, Genêt C, Sabatier F, Bonnieu A, Cousin X. 2006. Retinoic acid activates myogenesis in vivo through Fgf8 signalling. *Dev Biol* **289:** 127–140.

Hernandez RE, Putzke AP, Myers JP, Margaretha L, Moens CB. 2007. Cyp26 enzymes generate the retinoic acid response pattern necessary for hindbrain development. *Development* **134:** 177–187.

Houston DW, Wylie C. 2005. Maternal *Xenopus* Zic2 negatively regulates Nodal-related gene expression during anteroposterior patterning. *Development* **132:** 4845–4855.

Hyatt GA, Schmitt EA, Marsh-Armstrong NR, Dowling JE. 1992. Retinoic acid-induced duplication of the zebrafish retina. *Proc Natl Acad Sci* **89:** 8293–8297.

Hyatt GA, Schmitt EA, Marsh-Armstrong N, McCaffery P, Dräger UC, Dowling JE. 1996. Retinoic acid establishes ventral retinal characteristics. *Development* **122:** 195–204.

Inoue T, Ota M, Ogawa M, Mikoshiba K, Aruga J. 2007a. Zic1 and Zic3 regulate medial forebrain development through expansion of neuronal progenitors. *J Neurosci* **27:** 5461–5473.

Inoue T, Ota M, Mikoshiba K, Aruga J. 2007b. Zic2 and Zic3 synergistically control neurulation and segmentation of paraxial mesoderm in mouse embryo. *Dev Biol* **306:** 669–684.

Kimmel CB, Ballard WW, Kimmel SR, Ullmann B, Schilling TF. 1995. Stages of embryonic development of the zebrafish. *Dev Dyn* **203:** 253–310.

Krauss S, Johansen T, Korzh V, Moens U, Ericson JU, Fjose A. 1991a. Zebrafish pax[zf-a]: A paired box-containing gene expressed in the neural tube. *EMBO J* **10:** 3609–3619.

Krauss S, Johansen T, Korzh V, Fjose A. 1991b. Expression of the zebrafish paired box gene pax[zf-b] during early neurogenesis. *Development* **113:** 1193–1206.

Krauss S, Concordet JP, Ingham PW. 1993. A functionally conserved homolog of the *Drosophila* segment polarity gene hh is expressed in tissues with polarizing activity in zebrafish embryos. *Cell* **75:** 1431–1444.

Kudoh T, Wilson SW, Dawid IB. 2002. Distinct roles for Fgf, Wnt and retinoic acid in posteriorizing the neural ectoderm. *Development* **129:** 4335–4346.

Langenau DM, Jette C, Berghmans S, Palomero T, Kanki JP, Kutok JL, Look AT. 2005. Suppression of apoptosis by bcl-2 overexpression in lymphoid cells of transgenic zebrafish. *Blood* **105:** 3278–3285.

Lewis KE, Concordet JP, Ingham PW. 1999. Characterisation of a second patched gene in the zebrafish *Danio rerio* and the differential response of patched genes to Hedgehog signalling. *Dev Biol* **208:** 14–29.

Lowe LA, Yamada S, Kuehn MR. 2001. Genetic dissection of nodal function in patterning the mouse embryo. *Development* **128:** 1831–1843.

Lupo G, Liu Y, Qiu R, Chandraratna RA, Barsacchi G, He RQ, Harris WA. 2005. Dorsoventral patterning of the *Xenopus* eye: A collaboration of Retinoid, Hedgehog and FGF receptor signalling. *Development* **132:** 1737–1748.

Lupo G, Harris WA, Lewis KE. 2006. Mechanisms of ventral patterning in the vertebrate nervous system. *Nat Rev Neurosci* **7:** 103–114.

Macdonald R, Barth KA, Xu Q, Holder N, Mikkola I, Wilson SW. 1995. Midline signalling is required for Pax gene regulation and patterning of the eyes. *Development* **121:** 3267–3278.

Maden M, Blentic A, Reijntjes S, Seguin S, Gale E, Graham A. 2007. Retinoic acid is required for specification of the ventral eye field and for Rathke's pouch in the avian embryo. *Int J Dev Biol* **51:** 191–200.

Mathieu J, Barth A, Rosa FM, Wilson SW, Peyriéras N. 2002. Distinct and cooperative roles for Nodal and Hedgehog signals during hypothalamic development. *Development* **129:** 3055–3065.

Mathieu J, Griffin K, Herbomel P, Dickmeis T, Strähle U, Kimelman D, Rosa FM, Peyriéras N. 2004. Nodal and Fgf pathways interact through a positive regulatory loop and synergize to maintain mesodermal cell populations. *Development* **131:** 629–641.

Matsunaga E, Shiota K. 1977. Holoprosencephaly in human embryos: Epidemiologic studies of 150 cases. *Teratology* **16:** 261–272.

Maves L, Jackman W, Kimmel CB. 2002. FGF3 and FGF8 mediate a rhombomere 4 signaling activity in the zebrafish hindbrain. *Development* **129:** 3825–3837.

Mui SH, Kim JW, Lemke G, Bertuzzi S. 2005. Vax genes ventralize the embryonic eye. *Genes & Dev* **19:** 1249–1259.

Müller F, Albert S, Blader P, Fischer N, Hallonet M, Strähle U. 2000. Direct action of the nodal-related signal cyclops in induction of sonic hedgehog in the ventral midline of the CNS. *Development* **127:** 3889–3897.

Nagai T, Aruga J, Minowa O, Sugimoto T, Ohno Y, Noda T, Mikoshiba K. 2000. Zic2 regulates the kinetics of neurulation. *Proc Natl Acad Sci* **97:** 1618–1623.

Negron JF, Lockshin RA. 2004. Activation of apoptosis and caspase-3 in zebrafish early gastrulae. *Dev Dyn* **231:** 161–170.

Perz-Edwards A, Hardison NL, Linney E. 2001. Retinoic acid-mediated gene expression in transgenic reporter zebrafish. *Dev Biol* **229:** 89–101.

Rebagliati MR, Toyama R, Haffter P, Dawid IB. 1998a. cyclops encodes a nodal-related factor involved in midline signalling. *Proc Natl Acad Sci* **95:** 9932–9937.

Rebagliati MR, Toyama R, Fricke C, Haffter P, Dawid IB. 1998b. Zebrafish nodal-related genes are implicated in axial patterning and establishing left–right asymmetry. *Dev Biol* **199:** 261–272.

Rissi M, Wittbrodt J, Délot E, Naegeli M, Rosa FM. 1995. Zebrafish Radar: A new member of the TGF-β superfamily defines dorsal regions of the neural plate and the embryonic retina. *Mech Dev* **49:** 223–234.

Rohr KB, Schulte-Merker S, Tautz D. 1999. Zebrafish zic1 expression in brain and somites is affected by BMP and hedgehog signalling. *Mech Dev* **85:** 147–159.

Rohr KB, Barth KA, Varga ZM, Wilson SW. 2001. The nodal pathway acts upstream of hedgehog signalling to specify ventral telencephalic identity. *Neuron* **29:** 341–351.

Saijoh Y, Adachi H, Sakuma R, Yeo CY, Yashiro K, Watanabe M, Hashiguchi H, Mochida K, Ohishi S, Kawabata M, et al. 2000. Left–right asymmetric expression of lefty2 and nodal is induced by a signalling pathway that includes the transcription factor FAST2. *Mol Cell* **5:** 35–47.

Sampath K, Rubinstein AL, Cheng AM, Liang JO, Fekany K, Solnica-Krezel L, Korzh V, Halpern ME, Wright CV. 1998. Induction of the zebrafish ventral brain and floorplate requires cyclops/nodal signalling. *Nature* **395:** 185–189.

Sanek NA, Grinblat Y. 2008. A novel role for zebrafish zic2a during forebrain development. *Dev Biol* **317:** 325–335.

Schier AF, Neuhauss SC, Helde KA, Talbot WS, Driever W. 1997. The one-eyed pinhead gene functions in mesoderm and endoderm formation in zebrafish and interacts with no tail. *Development* **124:** 327–342.

Schneider RA, Hu D, Rubenstein JL, Maden M, Helms JA. 2001. Local retinoid signaling coordinates forebrain and facial morphogenesis by maintaining FGF8 and SHH. *Development* **128:** 2755–2767.

Shanmugalingam S, Houart C, Picker A, Reifers F, Macdonald R, Barth A, Griffin K, Brand M, Wilson SW. 2000. Ace/Fgf8 is required for forebrain commissure formation and patterning of the telencephalon. *Development* **127:** 2549–2561.

Takamiya M, Campos-Ortega JA. 2006. Hedgehog signalling controls zebrafish neural keel morphogenesis via its level-dependent effects on neurogenesis. *Dev Dyn* **235:** 978–997.

Take-uchi M, Clarke JD, Wilson SW. 2003. Hedgehog signalling maintains the optic stalk-retinal interface through the regulation of Vax gene activity. *Development* **130:** 955–968.

Varga ZM, Wegner J, Westerfield M. 1999. Anterior movement of ventral diencephalic precursors separates the primordial eye field in the neural plate and requires cyclops. *Development* **126:** 5533–5546.

Walshe J, Mason I. 2003. Unique and combinatorial functions of Fgf3 and Fgf8 during zebrafish forebrain development. *Development* **130:** 4337–4349.

Warr N, Powles-Glover N, Chappell A, Robson J, Norris D, Arkell RM. 2008. Zic2-associated holoprosencephaly is caused by a transient defect in the organizer region during gastrulation. *Hum Mol Genet* **17:** 2986–2996.

White RJ, Nie Q, Lander AD, Schilling TF. 2007. Complex regulation of cyp26a1 creates a robust retinoic acid gradient in the zebrafish embryo. *PLoS Biol* **5:** e304. doi: 10.1371/journal.pbio.0050304.